OPTIMAL CONTROL OF COMPRESSIBLE WAKE FLOW USING PLASMA ACTUATORS BASED ON INPUT-OUTPUT ANALYSIS

Xu Zhang, Deli Li, Guangrui Sun
School of Energy Science and Engineering
Harbin Institute of Technology
Harbin, China, 150001
zhangxu36@stu.hit.edu.cn, lideli@stu.hit.edu.cn, g.sun@hit.edu.cn

ABSTRACT

Plasma actuators provide an effective means of flow control without altering aerodynamic geometry, yet the amplification mechanisms underlying their optimal actuation in compressible wakes remain insufficiently understood. In the present work, resolvent analysis is employed to investigate the linear input-output amplification between forcing and response for subsonic compressible flow past a square cylinder. Plasma actuation is represented using both global forcing and localized Gaussian body forcing, and the effects of Reynolds number, Mach number, and forcing location are examined systematically. Using this framework, we show that the square-cylinder wake is governed by a single dominant frequency-selective amplification mechanism over the parameter range considered. At low Mach number, the optimal resolvent response closely matches the critical global instability mode. Varying the Mach number preserves the same dominant branch, but shifts the optimal frequency toward lower values and changes the amplification level. For localized Gaussian body forcing, the same underlying mechanism remains dominant, and the top forcing configuration yields the strongest local amplification. The present results show that input-output analysis provides a physically interpretable framework for identifying the dominant amplification mechanism and for assessing the effectiveness of plasma-actuator forcing in compressible wakes.

INTRODUCTION

Plasma actuators provide an attractive means of flow control because they can modify the flow without altering the aerodynamic geometry (Cattafesta & Sheplak, 2011). Owing to this feature, they have been widely studied for applications such as drag reduction, separation control, and noise mitigation (Abe *et al.*, 2023; Zhu *et al.*, 2026). Plasma actuators have been successfully used to suppress laminar flow separation in supersonic flows by generating local heating and entraining high-momentum fluid, yet the mechanisms that amplify actuator forcing into large-scale flow responses remain unclear in compressible wakes (Chen *et al.*, 2022). Lakshmi Narasimha Prasad & Unnikrishnan (2024) numerically investigates the noise reduction mechanism of a Mach 1.5 rectangular jet using localized arc filament plasma actuators. The results show that the azimuthal actuation pattern M2 achieves the best noise reduction of up to 2.6 dB by suppressing high-energy supersonic modes and enhancing low-radiation helical modes, with negligible influence on the mean flow. For bluff-body wakes, however, especially in compressible flows, the mechanisms by which actuator forcing is amplified into large-scale flow responses remain insufficiently understood. A clearer physical description of these amplification processes is needed in order to guide the design of effective actuation strategies.

Resolvent analysis provides a useful input-output framework for this purpose. By linearizing the Navier–Stokes equations about a given base flow, it quantifies how external forcing is amplified into flow response and identifies the most amplified forcing-response structures. Such a framework is particularly attractive for model-based flow control (Jovanović, 2021). Recent studies have combined global resolvent analysis with spectral proper orthogonal decomposition (SPOD) and successfully applied them to the design of optimal forcing height and frequency for plasma actuators on airfoil surfaces, validating the effectiveness of this approach in model-based active flow control (Shi *et al.*, 2026). Nevertheless, its application to plasma-actuator design in compressible bluff-body wakes is still limited, especially regarding how the dominant amplification mechanism depends on Reynolds number, Mach number, and actuator placement. In addition, while previous studies have often employed simplified actuator representations, the influence of localized forcing distribution on the optimal response structure has not been systematically clarified for compressible wake flows.

In the present work, we apply resolvent analysis to subsonic compressible flow past a square cylinder, with plasma actuation modeled as both global forcing and localized Gaussian body forcing. The effects of Reynolds number, Mach number, and forcing location on the gain characteristics and optimal forcing-response modes are examined systematically. The results show that the wake is governed by a single dominant amplification mechanism, while Mach number and forcing location mainly modify the optimal frequency and amplification level rather than the underlying input-output structure.

METHODS

The current work focuses on compressible flow, whose governing equations under external forcing can be expressed as

$$\frac{\partial \boldsymbol{q}}{\partial t} = \mathscr{L}(\boldsymbol{q}) + \boldsymbol{B}\boldsymbol{f}, \quad \boldsymbol{y} = \boldsymbol{C}\boldsymbol{q}, \tag{1}$$

where $\mathscr{L}$ denotes the linearized Navier-Stokes operator based on steady or time-averaged base flow, $q = (\rho, \rho\boldsymbol{u}, \rho e)$ is the state vector, and $\boldsymbol{f}$ represents the external forcing. A calorically perfect gas is considered in the present study, and the viscosity μ is calculated using Sutherland's law. Within the framework of input–output analysis (Jovanović, 2021), $\boldsymbol{B}$ is the input operator that defines how the forcing is applied, while $\boldsymbol{C}$ is the output operator that maps the state to the response of interest for optimization. Resolvent analysis offers an input–output framework well-suited for model-based flow control, in which the Navier–Stokes equations are linearized around a base flow, and the resulting linear operator quantifies how external forcing inputs are amplified into flow response outputs, offering direct guidance to the design of optimal actuation strategies.

Specifically, consider harmonic forcing through a temporal Fourier transform of forcing and response, such that $\boldsymbol{f} = \hat{\boldsymbol{f}} e^{-i\omega t}$, leading to an input-output relationship given by

$$\hat{\boldsymbol{q}} = \boldsymbol{C}(-i\omega \boldsymbol{I} - \mathscr{L})^{-1}\boldsymbol{B}\hat{\boldsymbol{f}} = \boldsymbol{H}_\omega \hat{\boldsymbol{f}}, \qquad (2)$$

where $\boldsymbol{H}_\omega$ is the resolvent operator which acts as a transfer function between the forcing and the response at frequency ω, and $\boldsymbol{I}$ denotes the identity matrix. In practice, the frequency of harmonic forcing can be regarded as analogous to that of a plasma actuator, which is typically driven by alternating current (AC) voltage (Suzen *et al.*, 2005; Benard & Moreau, 2010).

Following a recent work of Kawai *et al.* (2018), the plasma actuator is modeled using a simplified body-force representation, which is incorporated through the input operator

$$\boldsymbol{B}(x,y,k_z) = A s_z \exp\left[-\frac{(x-x_0)^2}{2s_x^2} - \frac{(y-y_0)^2}{2s_y^2} - \frac{s_z^2 k_z^2}{2}\right], \qquad (3)$$

where A is the amplitude of the Gaussian distribution. A Fourier transform is applied in the homogeneous z direction in order to facilitate the bi-global resolvent analysis. The center and the shape of the Gaussian distribution are controlled by (x_0, y_0, k_z) and (s_x, s_y, s_z), respectively, where k_z is the spanwise wavenumber. Note that in the current work, no constraints are imposed on the response mode, i.e., $\boldsymbol{C} = \boldsymbol{I}$. The optimal energy amplification strategy induced by the aforementioned plasma actuators can be evaluated using singular value decomposition (SVD) (Rolandi *et al.*, 2024), where singular values give the gains, the left and right singular vectors correspond to the response and forcing modes, and disturbance energy is measured by Chu's energy norm (Chu, 1965).

In practice, the numerical simulations and resolvent analyses are computed based on an open-source finite-element code FreeFem++ (Hecht, 2012). The primitive variables are discretized on an unstructured mesh generated by a Delaunay triangulation procedure with the built-in mesh generator Bamg. Quadratic $P2$ elements are used for the velocity components, while linear $P1$ elements are adopted for pressure, temperature, and density. The resulting nonlinear algebraic system is solved by a Newton-Raphson procedure, and the linear systems arising at each iteration are handled with the multifrontal sparse LU solver MUMPS (Amestoy *et al.*, 2001). The two-dimensional square cylinder has a side length of $D = 1$ and is centered at the origin. The computational domain is $x \in [-50, 100]$, $y \in [-40, 40]$, with a main region $x \in [-25, 70]$, $y \in [-20, 20]$, and the surrounding outer region is used as a sponge layer to damp outgoing disturbances and suppress reflections near the inlet, outlet, and the upper and lower boundaries, following Fani *et al.* (2018). A thorough sensitivity analysis of the domain size, sponge layer, and grid resolution has been performed for all cases considered in the present study.

RESULTS AND DISCUSSION

In the current work, resolvent analysis is performed for subsonic compressible flow past a square cylinder under different Reynolds and Mach numbers. The computational setup follows Kumar *et al.* (2021), with a uniform inflow at the inlet and symmetry boundary conditions at the top and bottom boundaries. The results below are organized to examine the Reynolds-number effect on the dominant gain branch, the Mach-number dependence of the optimal frequency and modal structure, and the influence of localized Gaussian body forcing on the input-output amplification mechanism.

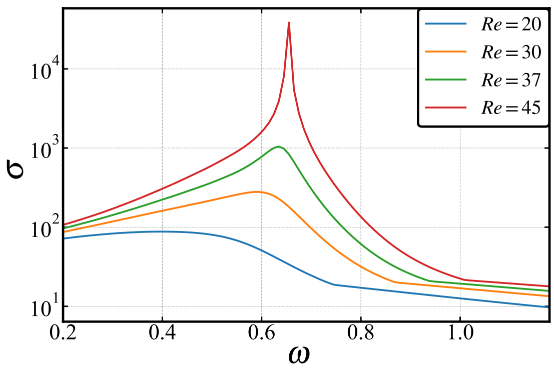

Figure 1: Resolvent gains at different Reynolds numbers at Mach number $Ma = 0.1$.

The results for weakly compressible flow at $Ma = 0.1$ are first examined, as shown in Figure 1. The gain–ω curves exhibit a single pronounced resonant peak for all Reynolds numbers considered, indicating that the flow response is governed by an unique dominant frequency. As the Reynolds number increases, the maximum gain rises rapidly, whereas the peak frequency remains confined to a narrow range with only limited variation. Nevertheless, despite little change in the characteristic frequency of the dominant mode as Re increases, its amplification becomes progressively stronger. In other words, the main effect of increasing Re is a progressive strengthening of the same dominant mode, rather than a shift in its dominant frequency. In particular, the largest amplification occurs at the critical Reynolds number $Re_c \approx 45$, consistent with the onset of instability predicted by linear stability analysis. At the weakly compressible condition, the critical frequency obtained from the stability analysis is 0.653, while the optimal frequency predicted by resolvent analysis under the same condition is 0.676. The close agreement between these two values indicates that the most amplified resolvent response already captures the characteristic frequency of the critical instability mode. Therefore, consistent with the incompressible global stability results of Chiarini *et al.* (2021), the low-Mach-number square-cylinder wake is governed by a single frequency-selective structure whose amplification peaks near the critical condition.

Additionally, the dominant resolvent modes at $Ma = 0.1$ are compared with the global eigenmodes in Figure 2. The response and forcing modes nearly coincide with the global

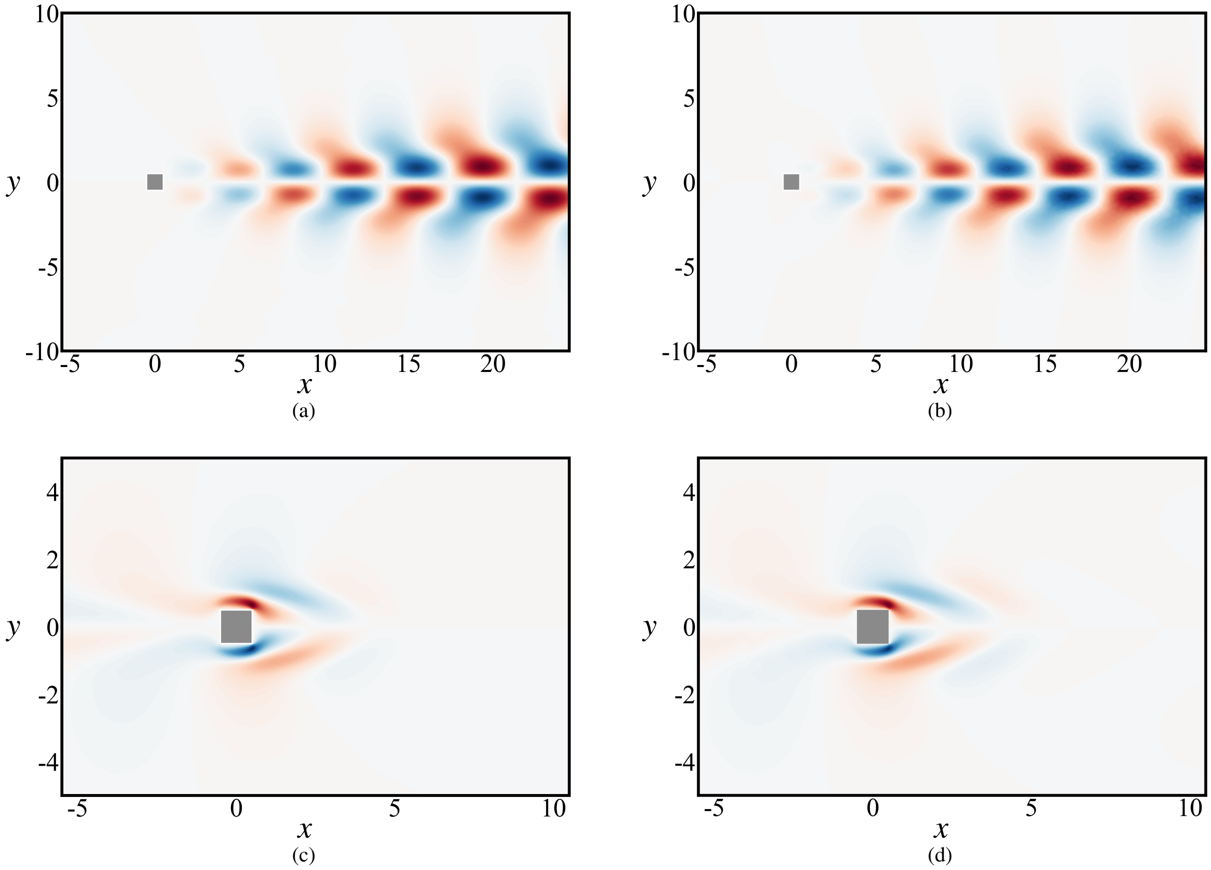

Figure 2: Comparison of stability modes (left) with resolvent modes (right) at Mach number $Ma = 0.1$ and the critical Reynolds number $Re_c = 45$: (a), (b) streamwise component of the direct and response modes, respectively; (c), (d) streamwise component of the adjoint and forcing modes, respectively.

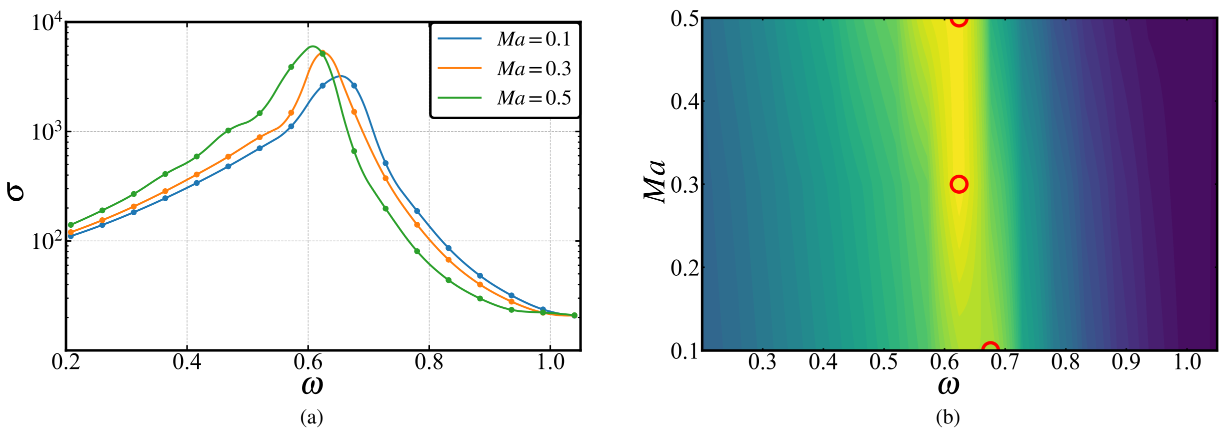

Figure 3: Resolvent analysis at different Mach numbers: (a) optimal amplification (gain) as a function of frequency for different Mach numbers; (b) contour map of the gain in the (ω, Ma) plane, where the peak frequencies identified from panel (a) are marked by red circles.

direct and adjoint eigenmodes, respectively. Therefore, at the transition threshold, the resolvent analysis and the linear stability analysis provide a consistent physical description of the same instability mechanism, namely a globally selected wake mode that first becomes unstable through the supercritical Hopf bifurcation. Specifically, the response mode displays an asymmetric structure that develops downstream, which is typical of the primary instability of wake flows. The adjoint mode and the forcing mode exhibit highly similar spatial distributions and are both concentrated in the vicinity of the square cylinder and the near-wake shear layers. The clear distinction between forcing and response regions suggests that the near-body region serves as the principal receptivity region, while the downstream wake contains the most amplified flow structures.

The effect of compressibility is further investigated in Figure 3. At $Re = 45 \approx Re_c$, the resolvent gain curves in panel (a) exhibit a single dominant peak for all Mach numbers considered, indicating that the flow response remains governed by a single dominant amplification mechanism at similar frequen-

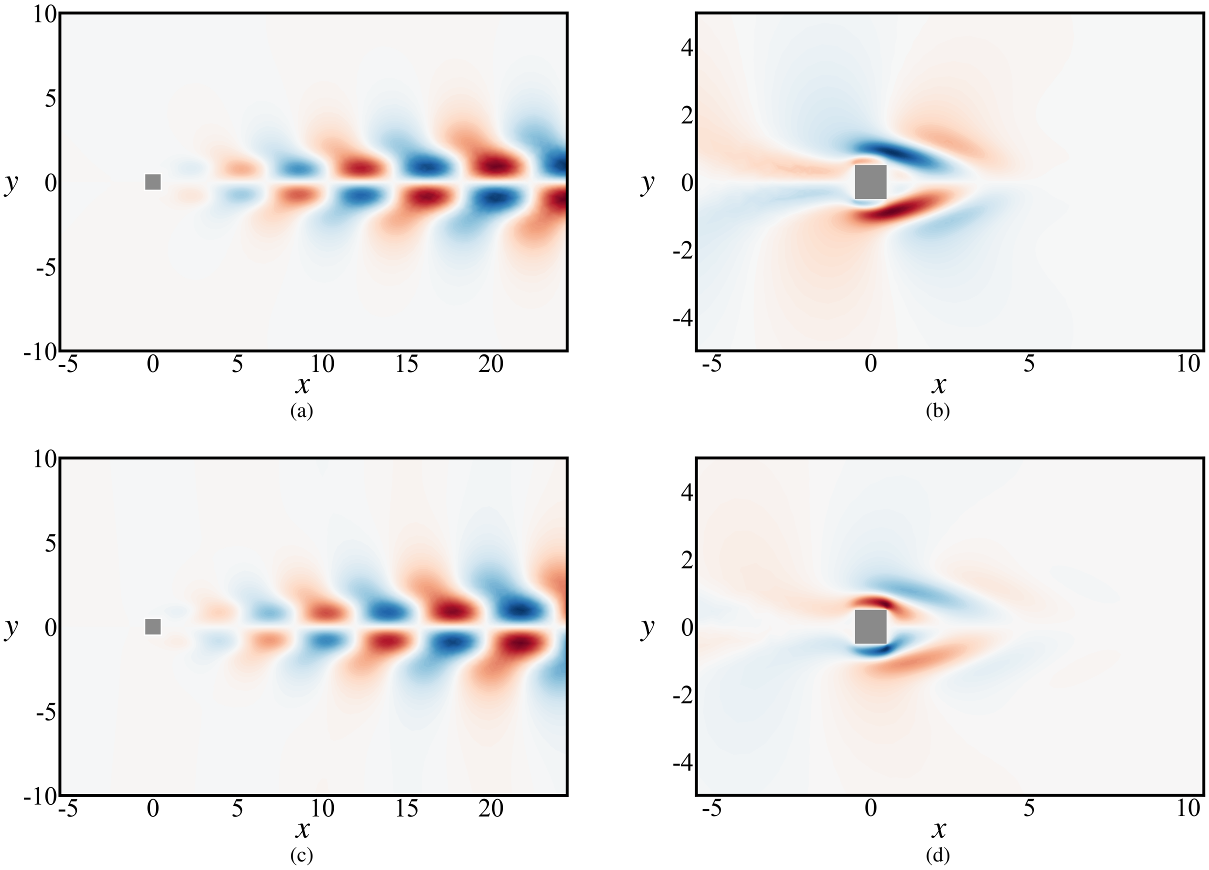

Figure 4: Comparison of streamwise components of resolvent modes at different Mach numbers: (a), (b) streamwise components of response and forcing modes, respectively, at $Ma = 0.3$, and (c), (d) streamwise components of response and forcing modes, respectively, at $Ma = 0.5$.

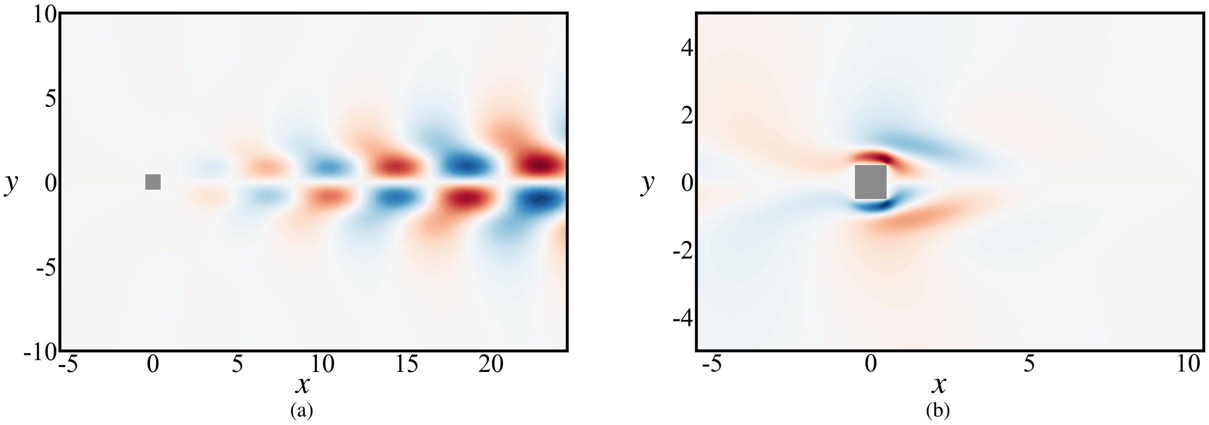

Figure 5: Streamwise components of resolvent modes at $Ma = 0.6$: (a) response mode, (b) forcing mode.

cies over the range of Mach numbers considered. The corresponding gain map in panel (b) further confirms that these peak frequencies lie on a continuous high-σ region in the (ω, Ma) plane, suggesting that the change of Ma mainly shifts the optimal frequency and modifies the amplification level along the same dominant branch. In particular, the maximum gain at $Ma = 0.5$ is almost twice that at $Ma = 0.1$, demonstrating that compressibility strengthens the dominant amplification while slightly shifting the optimal response toward lower frequencies. The trend is also confirmed in the spatial modes in Figure 4. Although the gain level and optimal frequency vary with Mach number, the response modes at $Ma = 0.3$ and $Ma = 0.5$ retain nearly the same downstream oscillatory wake structure, while the forcing modes in both cases remain concentrated around the square cylinder and the near-wake shear layers. This indicates that the dominant input-output organization is essentially unchanged with increasing Mach number. Specifically, the near-body region continues to act as the principal receptivity region, whereas the downstream wake remains the principal response region. In other words, the Mach number mainly affects the strength and selected frequency of the dominant resolvent branch, rather than introducing a qualitatively different amplification mechanism. In addition, at $Ma = 0.6$, the streamwise components of the optimal response and forc-

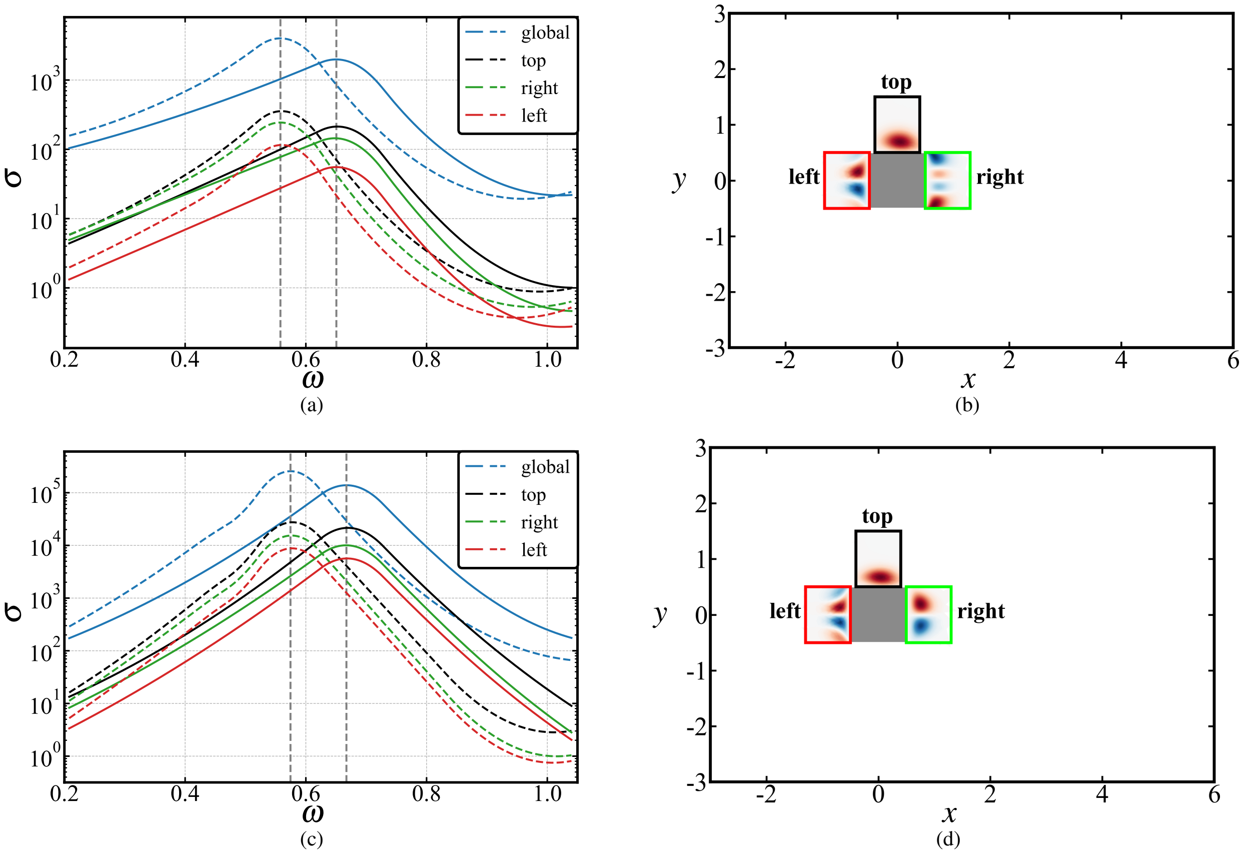

Figure 6: Results of 2-D input-output analysis with localized Gaussian body forcing: (a), (c) optimal amplification (gain) for global and localized Gaussian forcing at $Re = 45$ and $Re = 100$, respectively, with solid lines for $Ma = 0.1$ and dashed lines for $Ma = 0.6$; (b), (d) localized forcing modes at $Ma = 0.6$ for $Re = 45$ and $Re = 100$, respectively.

ing modes at $Re = 45$ are shown in Fig. 5(a,b). Similar to the low-Ma counterparts, the response mode exhibits a downstream oscillatory wake structure, whereas the forcing mode is localized in the vicinity of the square cylinder and the near-wake shear layers, indicating a clear spatial separation between the principal receptivity region and the principal response region.

Moreover, following the numerical study of Anzai *et al.* (2017) on flow control of a square cylinder using plasma actuators, three distinct forcing regions are considered on the left, right, and top boundaries, while the bottom boundary is identical to the top by symmetry. The plasma actuators are modeled according to equation (3) and incorporated into the input matrix of the resolvent analysis, enabling identification of the optimal forcing in the restricted regions from the viewpoint of nonmodal stability analysis (Schmid & Brandt, 2014). The corresponding input-output results are summarized in Figure 6. At the relatively low Reynolds number of $Re = 45$, the gain curves at different forcing regions are presented in panel (a), where solid lines denote $Ma = 0.1$ and dashed lines denote $Ma = 0.6$. According to the peak frequencies marked by the gray dashed lines, the dominant peak is located at $\omega = 0.651$ for $Ma = 0.1$ and at $\omega = 0.557$ for $Ma = 0.6$. Thus, at a fixed Reynolds number, increasing the Mach number leads to a decrease in the optimal frequency. In all cases, the global forcing yields the largest amplification. Among the localized Gaussian forcings, the top forcing is the most effective, followed by the right and left forcings. This indicates that the forcing location affects the amplification level, although the dominant response mechanism remains unchanged. The finding differs from the structural sensitivity analysis indicated by the adjoint modes (see, e.g., Figure 5(b)), which suggests that the wake region is most sensitive to perturbations. Such differences are expected, since the optimal gain obtained from resolvent analysis is determined from the perspective of energy amplification and does not rely on the assumption of exponential growth of infinitesimal perturbations. The result highlights that, even for the supercritical Hopf bifurcation examined in the present study, nonmodal stability analysis can offer fundamentally different predictions from eigenvalue-based modal analysis when providing guidance for flow control. Moreover, similar trends are also observed at $Re = 100$, as shown in panel (c). The dominant peak is located at $\omega = 0.666$ for $Ma = 0.1$ and at $\omega = 0.573$ for $Ma = 0.6$, while the overall gain level is substantially increased. The localized forcing modes shown in panel (b,d) further confirm that the Gaussian body forces remain concentrated in the near-body sensitive region. Overall, the current results indicate that localized Gaussian forcing preserves the same underlying input-output mechanism as the global forcing, while increasing Mach number shifts the optimal frequency toward lower values and modifies the amplification level.

CONCLUSIONS

In the present work, we investigated the linear input-output amplification characteristics of subsonic compressible flow past a square cylinder using resolvent analysis. Over the parameter range considered, the wake is governed by a single dominant amplification mechanism. Near the critical condition, the optimal resolvent response is closely related to the primary global instability mode, while the optimal forcing remains concentrated in the near-body and shear-layer region, indicating a clear separation between the main receptivity region and the main downstream amplification region. Increasing Mach number preserves the same dominant branch, but shifts the optimal frequency to lower values and modifies the amplification level, while the overall forcing and response structures remain qualitatively similar. The findings demonstrate that resolvent analysis provides a physically meaningful framework for identifying the dominant amplification process in compressible square-cylinder wakes.

Furthermore, following Anzai *et al.* (2017), the control performance of plasma actuators located at different edges of the square cylinder is also analyzed from a theoretical perspective based on the input-output framework. The results show that actuator placement mainly affects the achievable amplification level rather than the dominant wake mechanism. Among the localized Gaussian forcings, the top-edge actuator is consistently the most effective, followed by the right- and left-edge actuators, although the highest gain is still achieved with global forcing. In all cases, the dominant response structure remains essentially unchanged, indicating that different actuator locations do not alter the underlying amplification process. The results indicate that the effectiveness of plasma actuation depends strongly on actuator placement, with the top edge emerging as the most favorable control location among the configurations considered.

Overall, the present study demonstrates that resolvent analysis provides a physically interpretable framework for identifying the dominant amplification mechanism, the most effective forcing-response structures, and the relative performance of different localized actuation strategies in compressible square-cylinder wakes. Future work will extend the present analysis beyond the current linear and simplified forcing framework by incorporating more realistic plasma-actuator models, three-dimensional effects, spanwise-dependent forcing, and nonlinear input-output analysis that accounts for higher-order harmonic interactions (Rigas *et al.*, 2021). It would also be valuable to combine the present resolvent analysis with control-oriented optimization and high-fidelity simulations to assess the performance of the predicted optimal forcing strategies in practical flow-control configurations.

ACKNOWLEDGMENTS

The authors acknowledge financial support from the National Natural Science Foundation of China (grants 12402296 and 12272104) and the National Numerical Wind Tunnel Project (grant No. NNW2025-ZT3-16).

REFERENCES

Abe, Yoshiaki, Nonomura, Taku, Sato, Makoto, Aono, Hikaru & Fujii, Kozo 2023 Comparison of separation control mechanisms for synthetic jet and plasma actuators. *Actuators* **12** (8), 322.

Amestoy, Patrick R., Duff, Iain S., L'Excellent, Jean-Yves & Koster, Jacko 2001 A fully asynchronous multifrontal solver using distributed dynamic scheduling. *SIAM Journal on Matrix Analysis and Applications* **23** (1), 15–41.

Anzai, Yosuke, Fukagata, Koji, Meliga, Philippe, Boujo, Edouard & Gallaire, François 2017 Numerical simulation and sensitivity analysis of a low-reynolds-number flow around a square cylinder controlled using plasma actuators. *Physical Review Fluids* **2** (4).

Benard, N & Moreau, E 2010 Capabilities of the dielectric barrier discharge plasma actuator for multi-frequency excitations. *Journal of Physics D: Applied Physics* **43** (14), 145201.

Cattafesta, Louis N. & Sheplak, Mark 2011 Actuators for active flow control. *Annual Review of Fluid Mechanics* **43** (1), 247–272.

Chen, Zongnan, Hao, Jiaao & Wen, Chih-Yung 2022 Control of supersonic compression corner flow using a plasma actuator. *Physics of Fluids* **34** (7).

Chiarini, A., Quadrio, M. & Auteri, F. 2021 Linear stability of the steady flow past rectangular cylinders. *Journal of Fluid Mechanics* **929**.

Chu, Boa-Teh 1965 On the energy transfer to small disturbances in fluid flow (part i). *Acta Mechanica* **1** (3), 215–234.

Fani, A., Citro, V., Giannetti, F. & Auteri, F. 2018 Computation of the bluff-body sound generation by a self-consistent mean flow formulation. *Physics of Fluids* **30** (3).

Hecht, F. 2012 New development in freefem++. *Journal of Numerical Mathematics* **20** (3-4), 251–265.

Jovanović, Mihailo R. 2021 From bypass transition to flow control and data-driven turbulence modeling: An input–output viewpoint. *Annual Review of Fluid Mechanics* **53** (1), 311–345.

Kawai, Shigetaka, Bouwhuis, Thijs, Abe, Yoshiaki, Yakeno, Aiko, Nonomura, Taku, Aono, Hikaru, Oyama, Akira, Hoeijmakers, Harry W. M. & Fujii, Kozo 2018 Dominant parameters for maximum velocity induced by body-force models for plasma actuators. *Theoretical and Computational Fluid Dynamics* **32** (6), 805–820.

Kumar, Nitin, Tejyan, Sachin, Chamoli, Sunil & Kumar Pant, Pawan 2021 A discrete linear stability analysis of two-dimensional laminar flow past a square cylinder. *WSEAS TRANSACTIONS ON FLUID MECHANICS* **16**, 109–119.

Lakshmi Narasimha Prasad, Anirudh & Unnikrishnan, S. 2024 Noise mitigation in rectangular jets through plasma actuator-based shear layer control. *Journal of Fluid Mechanics* **979**.

Rigas, Georgios, Sipp, Denis & Colonius, Tim 2021 Nonlinear input/output analysis: application to boundary layer transition. *Journal of Fluid Mechanics* **911**.

Rolandi, Laura Victoria, Ribeiro, Jean Hélder Marques, Yeh, Chi-An & Taira, Kunihiko 2024 An invitation to resolvent analysis. *Theoretical and Computational Fluid Dynamics* **38** (5), 603–639.

Schmid, Peter J. & Brandt, Luca 2014 Analysis of fluid systems: Stability, receptivity, sensitivity. *Applied Mechanics Reviews* **66** (2).

Shi, Xuan, Xu, Bin & Sullivan, Pierre E. 2026 Optimized global resolvent analysis to improve plasma actuator control over the airfoil surface. *AIAA Journal* **64** (3), 1329–1349.

Suzen, Y., Huang, G., Jacob, J. & Ashpis, D. 2005 Numerical simulations of plasma based flow control applications. In *35th AIAA Fluid Dynamics Conference and Exhibit*. American Institute of Aeronautics and Astronautics.

Zhu, Zihao, Cheng, Hongzhi & Duan, Penghao 2026 Flow separation control over a highly loaded compressor blade using a plasma actuator. *Chinese Journal of Aeronautics* **39** (4), 103883.